Novel approach to microscopic characterization of cryo formation in air voids of concrete

Peiman Azarsa & Rishi Gupta

July 2019

Novel Approach to Microscopic Characterization of Cryo Formation in Air Voids of Concrete

Peiman Azarsa[1], Dr. Rishi Gupta[2*]
[1] PhD Candidate, Department of Civil Engineering, University of Victoria, Victoria, Canada, azarsap@uvic.ca
[2] Associate Professor, Department of Civil Engineering, University of Victoria, Victoria, Canada, guptar@uvic.ca

*Corresponding author: Dr. Rishi Gupta (guptar@uvic.ca), Tel: +1 (250) 721 7033

Abstract

Portland Cement Concrete (PCC) production is one of the major contributor to atmospheric Carbon Dioxide (CO_2) emission. Geopolymer Concrete (GPC) as an alternative construction material has the potential to reduce CO_2 emissions while creating durable structures. Freezing and thawing is an exemplary concrete deterioration mechanism that can cause widespread damage in concrete structures. Concrete structures exposed to freeze-thaw cycles delaminate due to expansive stresses induced when liquid converts to ice. There are numerous theoretical studies that have been done focused on capturing the effect of freeze-thaw cycles on microstructure of PCC. However, there is limited and no experimental work reported on cryo formation inside the air voids of PCC and GPC respectively. The main issue here is that most of the scanning electron microscopic devices cannot maintain the low temperature required to capture an image from a frozen sample. The amount of internal stress due to cryo formation and temperature range of cryo formation can be determined by investigation of morphology of the cryo products. Hence, in this study attempts have been made to investigate the morphology of the cryo formation inside the microstructure of GPC using a 4-D Low Temperature Scanning Electron Microscopic (4D-LTSEM). GPC specimens were frozen at -180 ºC and were slowly sublimated to capture cryo creation in the paste. According to ASTM C666, nominal freezing temperature for PCC is -18 ºC. So, the microstructure of GPC at -18 ºC was investigated to find the applicability of ASTM C666 for paste tense. The results show that rate of cryo formation is slow from 0 ºC to -18 ºC indicating sufficient resistance of GPC when exposed to cold climates.

Keyword: Geopolymer concrete; Freeze-thaw; Cryo morphology; Low Temperature Scanning Electron Microscopic.

1. Introduction

Geopolymer Concrete (GPC) as a green material in the construction industry has brought a widespread of attention due to its ability to reduce CO_2 emission. GPC is an inorganic material

where cement is replaced with industrial by-product materials and is activated by alkaline solution (Davidovits, 2015). Freeze-thaw cycles in cold climate regions lead to cracks and spalls in the structure of GPC due to progressive expansion of its matrix. Deterioration increases as freeze-thaw cycles are reiterated, and the concrete structure gradually loses its durability (Mehta & Monteiro, 2014). Therefore, one of the challenges that can be highlighted in GPC related studies is freeze-thaw resistance of structure in sub-zero temperatures. Microscopic study of concrete plays a vital role in identification of nature of the binding between paste and aggregates. Consequently, this identification helps to researchers to increase performance of concrete under various conditions (Azarsa & Gupta, 2018). Since there is a few literatures reported on microstructure of GPC (Chindaprasirt, et al., 2009) (Hanjitsuwan, et al., 2017), this aspect of K-based GPC is investigated in this paper.

Powers (Powers, 1958) microscopically examined the effect of water on the interior walls of PCC and proposed the hydrostatic pressure theory of freeze-thaw failure deterioration. According to this theory, the conversion of water to ice creates 9% volumetric expansion and concrete fails if the hydrostatic pressure exceeds the tensile strength of the paste. Powers et al. (Powers & Helmuth, 1953) also proposed the osmotic pressure that the transformation of water to ice inside the large pores is faster than small pores. This solution concentration difference between large frozen pores and small unfrozen pores create osmotic pressure. So, the osmotic pressure damages the gel pores of the paste.

Hydration process creates lots of capillary and gel pores inside the microstructure of PCC. So, there is huge amounts of free spaces for water to penetrate through the saturated paste. However, water inside the capillary pores freezes below -12 ºC. While, the temperature of -78 ºC is needed to freeze water inside the gel pores. So, it can be concluded that frozen water inside the capillary pores cause the freeze-thaw failure damages of concrete (Yu, et al., 2017). Nevertheless, there is no literature reported on the domain of the freezing point in pores of GPC.

Air Entrained Admixture (AEA) is used for concrete mixtures exposed to the cold environments. AEA produces millions of tiny chambers for water to relieve internal pressure when the concrete experiences freeze-thaw cycles (Kosior-Kazberuka & Berkowskib, 2017). Sufficient amount of AEA is required for concrete matrix to resist frost actions. AEA improves workability of the concrete paste although ultimate strength of concrete paste decreases (Mehta & Monteiro, 2014).

More air voids in the microstructure of concrete mixture provide more spaces to relieve hydrostatic pressure and prevent deterioration to concrete mixture (H.S.Wong, et al., 2011) (Kabashi, et al., 2016). Currently, there are abundant theoretical and experimental studies used to determine freeze-thaw resistance of PCC (Ziaei-Nia, et al., 2018) (Shang & Yi, 2013). However, no experimental work is reported on characterizing cryo formation in microstructure of GPC due to unavailability of 4D Low Temperature Scanning Electron Microscopic (4D-LTSEM) equipment.

Sun and Wu (Sun & Wu, 2013) investigated the effect of AEA on freeze-thaw resistance of fly-ash mortar and Ordinary Portland Cement (OPC) in accordance with ASTM C666 (ASTM C666, 2015). The mass loss and dynamic modulus retention of four compositions (OPC without AEA, OPC with AEA, fly-ash mortar without AEA and fly-ash mortar with AEA) were measured after 300 freeze-thaw cycles. Results showed that OPC without AEA subjected to the greater mass loss, while fly-ash with and without AEA gained mass after 300 cycles. AEA-based fly-ash mortar indicated a dynamic modulus loss of 6.8%, while Non-AEA-based fly-ash mortar lost 8.4% of the compressive strength after 300 cycles of freeze-thaw. The results also showed that Non-AEA-based OPC resulting in a strength loss of about 20% and AEA-based OPC had a final loss of only 5% after 300 cycles.

Since there is no research reported on the in-situ investigation of cryo formation of GPC, this research is targeted to experimentally and deeply investigate the morphology of cryo formation inside the entrained air voids of GPC matrix to have a comprehensive understanding of the extent of the microstructure of GPC paste exposed to the freeze-thaw cycles. Traditional microscopic devices are not able to maintain the temperature for a long enough period of time. So, tiny samples are expected to be warmed very quickly in the testing chamber. In this regard, 4D-LTSEM was used to take high-resolution images from ice propagation inside air voids of the GPC paste. 4D-LTSEM is setup to image tiny specimens kept under frozen conditions. This equipment has a temperature controlled stage so that the specimens can be held from -180 ºC to +100 ºC. Consequently, there is an opportunity to observe cryo products in air voids at a freshly fractured cross section.

2. Research contribution

Freeze-thaw resistance is a very critical characteristic of concrete when it is exposed to an aggressive environment. GPC structures located in cold environments can get damaged by freeze-thaw cycles during their life span. Hence, it is very important to study the microstructure

of the paste in the frozen condition giving an insight into the cryo morphology in the air-voids of GPC. This is important as the morphology can dictate the amount of internal stresses caused in the paste and indicate the temperature range when substantial amount of cryo products start to form in the microstructure of the mixture. There is limited work that focuses on investigation of cryo morphology in entrained air voids of traditional concrete (Wang, et al., 1996) (Corr, et al., 2002) (Monteiro, et al., 2006) but no research has been reported on formation of cryo products in air voids of GPC. This paper presents novelty focused on study of mechanism of cryo creation in the air-voids of GPC by using 4D-LTSEM.

3. Experimental work

3.1. Fly-ash and bottom-ash

In this study, GPC made by a combination of class F fly-ash and bottom-ash were used to investigate the effect of sub-zero conditions on microstructure of the paste. Lafarge Canada Inc. provided the fly-ash and bottom-ash for this study. Lafarge Canada Inc. used X-Ray Diffraction (XRD) technique to identify and characterise the chemical elements of fly-ash and bottom-ash. Table.1 shows that SiO_2, Al_2O_3, MgO, CaO, Na_2O and K_2O are detected in chemical composition of both fly-ash and bottom-ash.

Table-1 Chemical Compositions of fly-ash and bottom-ash (Source: Lafarge Inc.'s report)

Properties	**Fly-ash (%)**	**Bottom-ash (%)**
SiO_2	47.1	60.11
Al_2O_3	17.4	14.35
Fe_2O_3	5.7	5.92
CaO	14	10.40
MgO	5.4	4.49
SO_3	0.8	0.10
LOI	0.19	0.00
Na_2O	N/A	2.232
K_2O	N/A	1.766
TiO_2	N/A	0.892

P_2O_5	N/A	0.200
Mn_2O_3	N/A	0.093

3.2. Morphology of fly-ash and bottom-ash

The morphology analysis of the two industrial by-products are performed by using Scanning Electron Microscopy (SEM) to obtain more details about the microstructure of raw fly-ash and bottom-ash. Both materials were analysed under 16.0mm×1.20K magnification.

Figure.1 shows that fly-ash consists of spherical particles with a regular smooth texture, showing that fly-ash particles were subjected to the high temperatures during coal combustion in furnace (Yu, et al., 2012). As it is reported, the particle size of fly-ash is about 1 to 20 µm with average size of 10 µm (Davidovits, 2015).

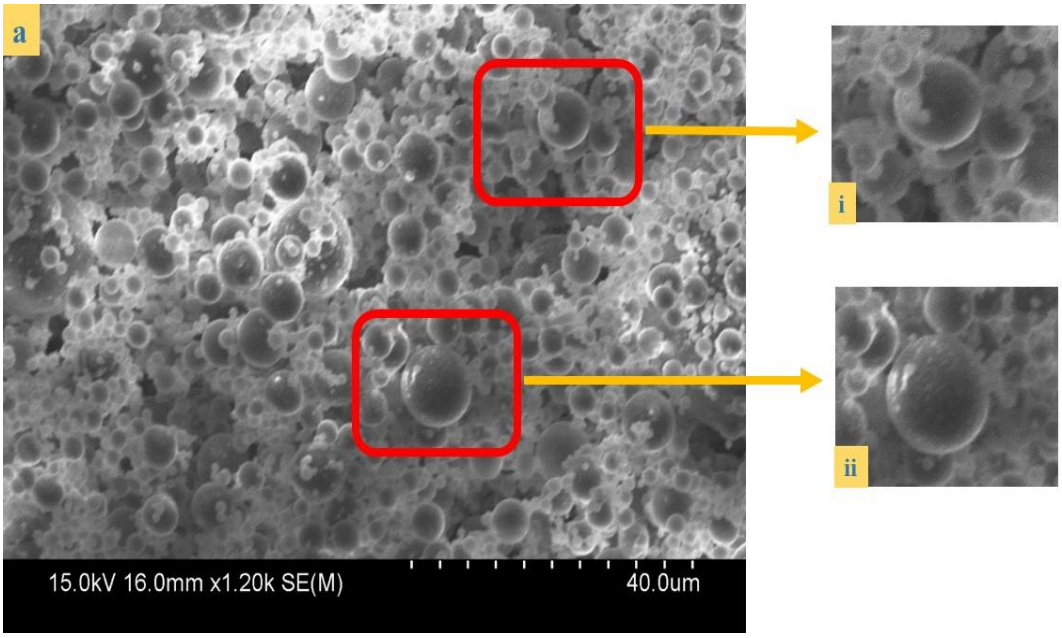

Figure 1. SEM image of fly-ash particle

(i)&(ii) Random areas

The SEM image of the bottom-ash (Figure.2) indicates both regular and irregular shaped particles. Two particles shown in the red rectangle were randomly selected to measure the size of regular and irregular shapes grains. Mal'chik et al. (Mal'chik, et al., 2015) investigated the chemical content and particle size distribution of bottom-ash particles of 130 samples. The results show that the particle dimensions of bottom-ash vary from 10 to 100 µm. In current study, the mean size of the rounded shape (Figure. 2 (i)) is 58.53µm. The average height and

width of the irregular shaped particle (Figure. 2 (ii)) is 22.59 and 12.78μm respectively. A comparison between Figure.1 and Figure.2 shows that bottom-ash particles are coarser than fly-ash particles. These coarser particles cause lower reactivity when used in GPC.

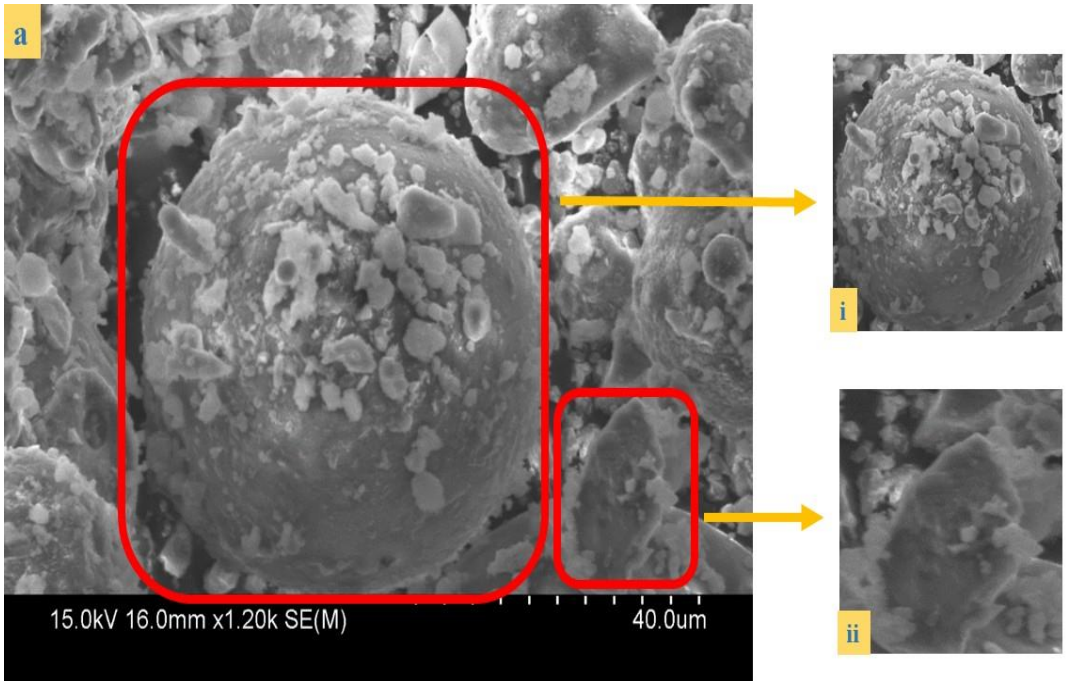

Figure 2. SEM image of bottom-ash particles

(i) Regular-shape
(ii) Irregular-shape

3.2. Alkaline solutions

Traditionally, sodium hydroxide (NaOH) and sodium silicate (Na_2SiO_3) have been used in production of GPC (Xie & Ozbakkaloglu, 2015) (Chindaprasirt, et al., 2009) (Mohamed, et al., 2016) but the combination of potassium hydroxide (KOH) and potassium silicate (K_2SiO_3) also can be used for the activation of fly-ash and bottom-ash. In the present study, powder form of K_2SiO_3 containing 85% K_2O-SiO_2 and 15% H_2O was supplied by PQ Corporation. The KOH with ≥85% purity was obtained from Sigma Aldrich, and mixed with water to make a solution with a concentration of 12 Molar. Alkaline activator ratio K_2SiO_3/KOH=1.48 was obtained for this study.

Initial trial experiments were performed to design a proper mix and to achieve a higher degree of workability (Gupta & Rathod, 2015) (Yang & Gupta, 2018) (Belforti, et al., 2017). Coarse aggregate and sand were locally obtained from a quarry in British Columbia, Canada with relative dry density of 2.671 and 2.713 respectively. The water absorption ratio of coarse aggregate and sand was measured 0.79% and 0.69% respectively. The nominal sizes of coarse aggregates was 12.5 mm. The total proportion of aggregates was measured 1800 kg/m^3.

The concentration of 12 in terms of Molarity (M) and 50:50% mass ratio of bottom-ash to fly-ash were selected to obtain a target strength of 35 MPa. As can be seen in Table 2, total density of mix is about 2400 kg/m^3. The total amount of by-products was obtained 388 kg/m^3 and total alkaline activator solution amount was obtained 211 kg/m^3. Hence, the ratio of alkaline activator solution to by-products was measured to 0.5 approximately. Table. 2 shows the mix design of GPC.

Table 2- Mix Design	**GPC**
Material	Content (Kg/m^3)
Fly-ash	194
Bottom-ash	194
Coarse aggregates	1170
Sand	630
KOH (12M)	85.16
K_2SiO_3	125.74
Water	38.71
Air Entrained Admixture	1.5 %

In the frozen condition, the deterioration of the GPC happens due to moisture freezing in air voids of mixture and subsequent expansion of the paste. The expansion force from the frozen water can exceed the tensile strength of the GPC and delaminate the paste. This phenomenon destructively affects the ultimate strength and durability of GPC and threatens the lifespan of a structure (Mehta & Monteiro, 2014). Generally, the resistance of GPC subjected to the freeze-thaw cycles is dependent on content, size and spacing of air content (Bakharev, et al., 2000). AEA as one of the surface active agent/ surfactant is basically used to relieve internal pressure and increase the freeze-thaw resistance of GPC. AEA entrained air bubbles in mixture by changing the surface tension of water and act at the air-water interface within the mixture. AEA consists of a hydrophilic head (polar) and a hydrophobic (radical) tail, by which it gets orientated into the air phase with the polar molecules inward toward the water (Mehta & Monteiro, 2014). AEA creates more tiny spaces for the expansion of ice by producing air bubbles with diameter ranging from 10 μm to 1mm (Bakharev, et al., 2000).

In this study, the air content of GPC was measured by pressure apparatus with a capacity of 0.25 ft^3 in accordance with ASTM C 231 (ASTM C231, 2015). The fresh GPC was poured in a pressure vessel in three layers. Each layer was consolidated by a 25 tamping rod-drop from a height of 30 mm. After dropping, the measurement in a pressure apparatus was conducted. The average air content of six samples of fresh AEA-based GPC was about 4.5±0.5%.

To produce GPC samples, dry materials were first mixed in a mixer for 1 minute. Then, KOH and K_2SiO_3 solution, already prepared (24 hrs before casting day), were added steadily to the mixture along with extra water for 3 minutes, followed by a 3 minutes rest period, followed by 2 minutes of final mixing. After molding, GPC samples were vibrated for 30 seconds to discharge the air bubbles to the surface. The samples were then kept at an ambient temperature for 24 hrs (approximate relative humidity range of 45% to 70% and approximate temperature range of 5ºC to 15ºC). The samples were demolded after 24 hrs and were steam cured at 80 ºC for 24 hrs (Belforti, et al., 2017).

A tiny chunk of the paste from the surface of 28-day cured GPC samples were taken to study the pore walls in the 4D-LTSEM cooling chamber. Liquid nitrogen was used to freeze the GPC specimens. 4D-LTSEM is designed to take images at very low temperature of upto -180 ºC. In this study, initially, the samples were frozen at a temperature of -180 ºC to take the images of cryo products and then the samples were slowly warmed in the chamber to take images from the exact same locations after the sublimation of ice.

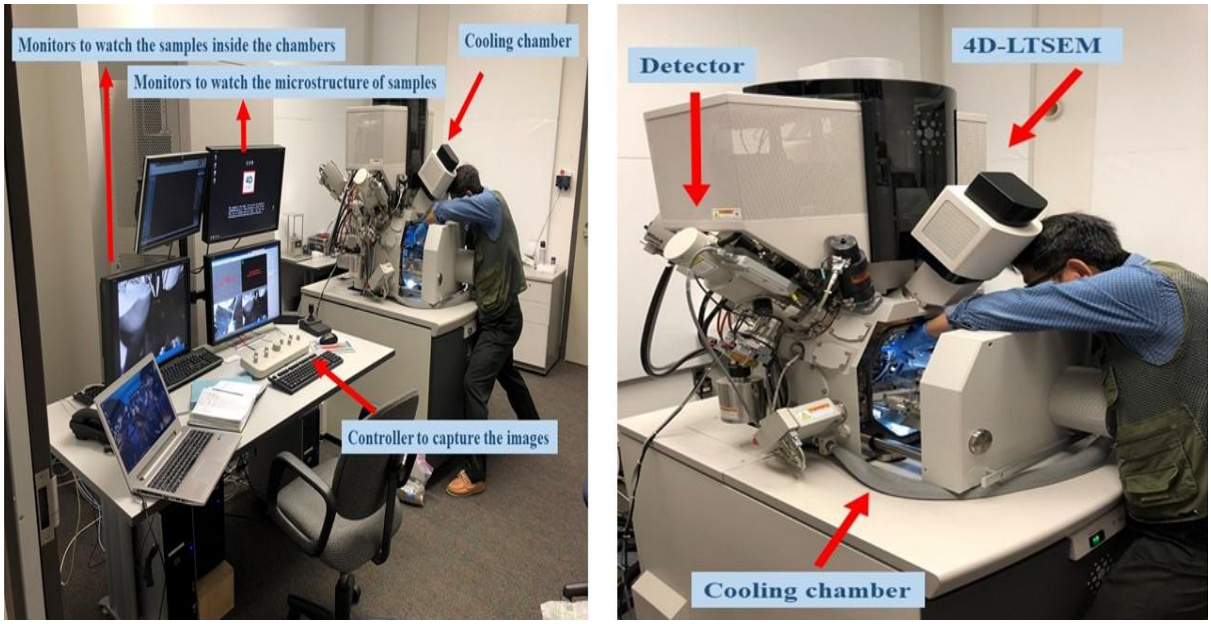

Figure 3. 4-D Low Temperature Scanning Electron Microscopic

The 4-D LTSEM (FEI Helios Nano-Lab Dual-Beam 650) is a combined field emission SEM and Focused Ion Beam (FIB) technology. It is designed to capture high resolution SEM images at low temperatures (up to -180 ºC) and high temperatures (up to +100 ºC). The equipment has low kV operation down to 500 V and up to 65 nA beam current. The main part of 4-D LTSEM shown in Figure. 3 is the cooling chamber. This chamber/stage is able to maintain the temperature for the specimen that needs to be tested at sub-zero temperature.

Isac-García et al. (Isac-García, et al., 2016) proposed that the rate of sublimation decrease when the pressure in the chamber becomes higher than the pressure of the ice. Sublimation continuously begins from external surface and migrates to inside the specimens. This phenomenon creates two different layers in a specimen, dry layer and frozen layer. The boundary of these two layer named "sublimation interface" or "ice interface" (Isac-García, et al., 2016). So, as it was suggested by Corr et al. (Corr, et al., 2002), in this study attempts have been made to keep the average chamber pressure at about 1.3^{-9} millibar to reduce the rate of sublimation of water from surface of specimen and to avoid creation of sublimation interface to detect the main ice morphology inside the air voids of GPC.

Additionally, in real environmental conditions, since the gas molecules sublimated from dry layer need to be fitted in the atmospheric gases, the process of sublimation is preferred to be slow in barometric pressure/atmospheric pressure (Isac-García, et al., 2016). ASTM C666 (ASTM C666, 2015) is also well-agreed with a longer transition period from freezing to thawing phase.

4. Results and discussion

Basically, the formation of the GPC paste is totally different from that in PCC which consequently leads to a different microstructure (Azarsa & Gupta, 2018) (Chindaprasirt, et al., 2009). Figure.4 is a micrograph of K-based GPC i.e. the SEM image at 600X magnification. The SEM image of K-based GPC shows a large proportion of reacted particles. So, relatively dense matrix can be seen in microstructure of GPC. It also can be observed that both bottom-ash and fly-ash particles are properly embedded into the paste. So, it means that GPC pastes were fully and uniformly cured.

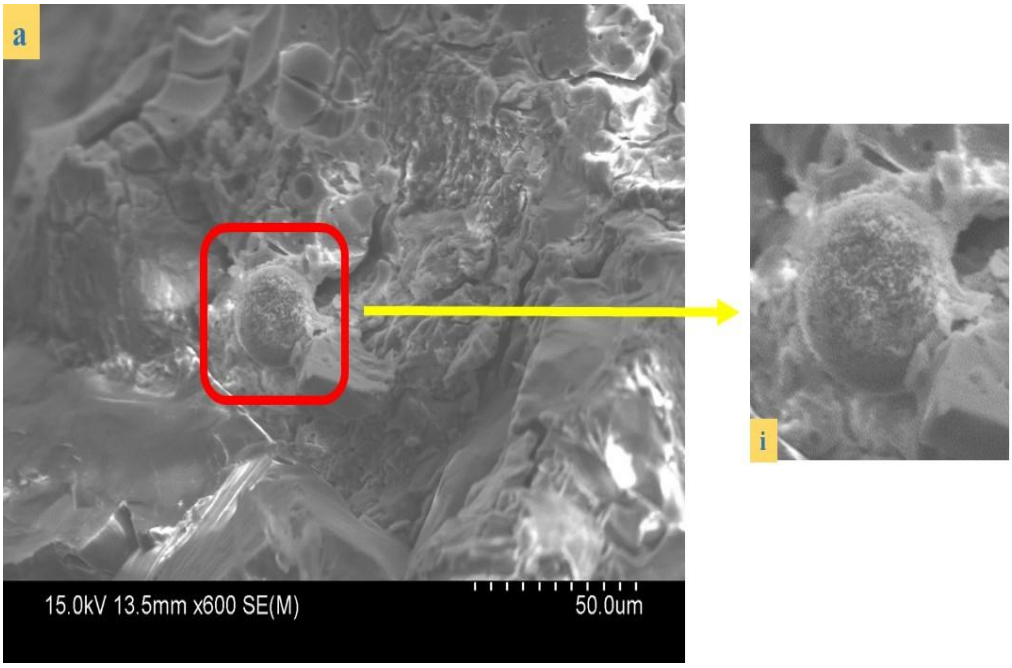

Figure 4. SEM image of GPC

From visual observation under the 4D-LTSEM, it was found that the air void structure of GPC is totally different from air voids reported for PCC (Corr, et al., 2002) (Monteiro, et al., 2006). Initially, the samples were frozen at the temperature of -180 ºC to take images of created cryo products and then the samples were warmed to take image after sublimation of cryo products. As can be seen in Figure. 5(a), the surface of paste is totally covered with cryo products at temperature of -180 ºC and most of the air voids are invisible. So, all the voids are probably clogged with cryo products and possibly the paste is subjected to significant expansion. Figure.5 (b) indicates the same area after sublimation of the cryo products at a temperature of about -70 ºC. At this temperature, due to the high freeze-resistance capacity of the air voids of GPC, most of cryo products disappeared and more voids are visible on the surface of the paste. The images taken at a temperature of -18 ºC -10 ºC (Figure.5 (c) and (d)) indicates that the surface of the paste is almost smooth and the voids are completely empty. The red rectangles in Figure.5 (c) and (d) were randomly selected to observe the rate of cryo products sublimation. As it can be seen, there is no evidence of cryo products inside the random area due to high freeze-resistance of the paste.

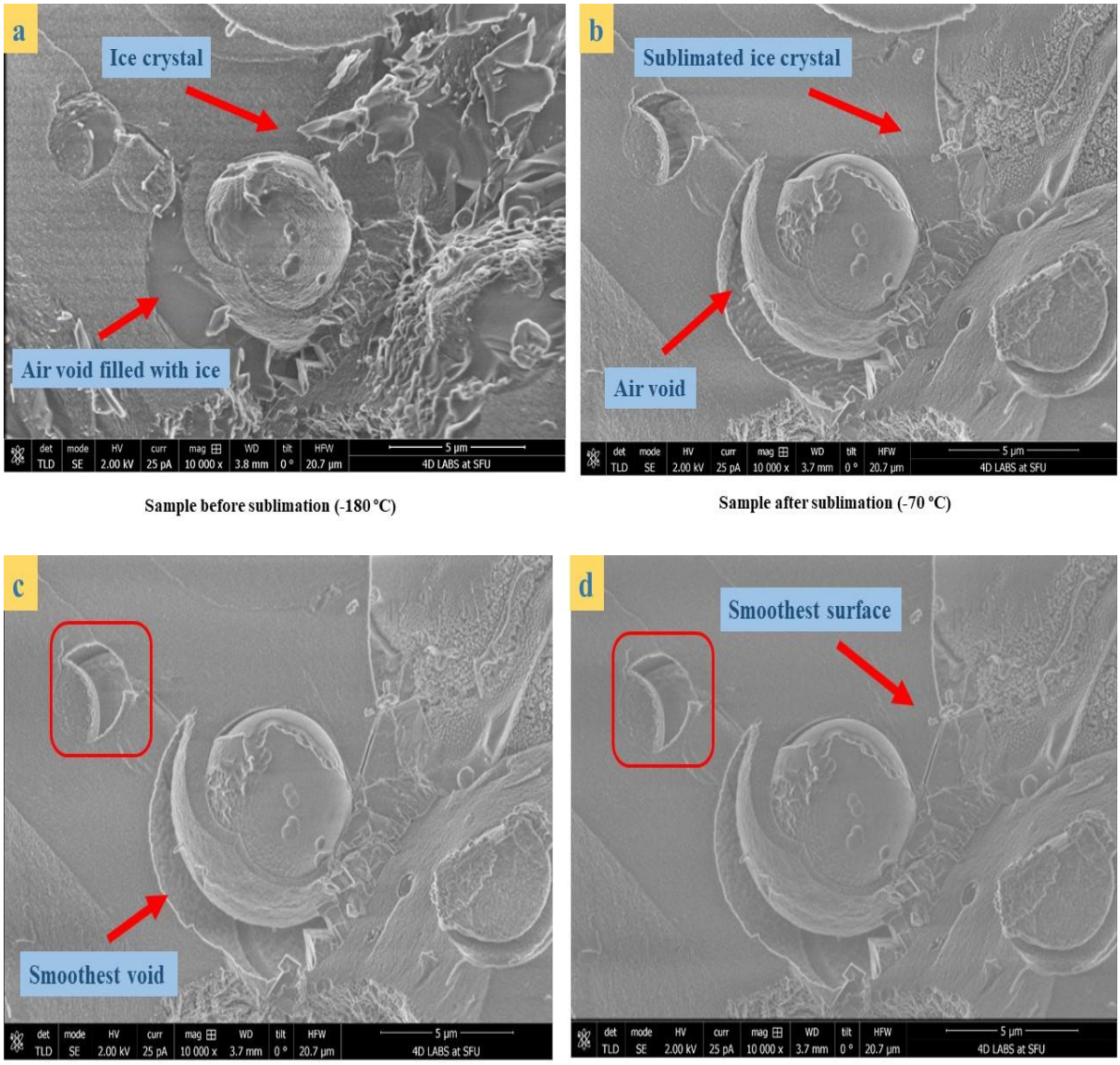

239 Sample before sublimation (-180 °C) Sample after sublimation (-70 °C)

240 Sample after sublimation (-18 °C) Sample after sublimation (-10 °C)

241 **Figure 5. 4D-LTSEM images of frozen GPC sample at following temperatures: (a) -180 °C, (b) -70 °C, (c) -18 °C and (d) -10 °C**

242 Generally, unlike the cryo formation in the air voids of PCC reported by David J. Corr (Corr,
243 et al., 2002), the ice on the surface of air voids formed non-discretely; ice covered the air voids
244 because the samples were immersed in the water to be fully-saturated. Based on the ASTM
245 C666 (ASTM C666, 2015), at the end of the cooling period (-18 ºC) the paste is still expected
246 to show proper strength. The comparison between the four micrographs in Figure. 5 show that
247 the rate of cryo formation from a temperature of 0 ºC to -10 ºC is same as cryo formation from
248 temperature of -10 ºC to -18 ºC. Hence, it can be concluded that only water inside the capillary
249 pores froze below -18 ºC. However, from visual observation, it was found that the rate of cryo
250 products sublimation decreased dramatically from -70 ºC to -18 ºC. It shows that the ice inside
251 the gel pores began to melt at a temperature of -70 ºC to -18 ºC.

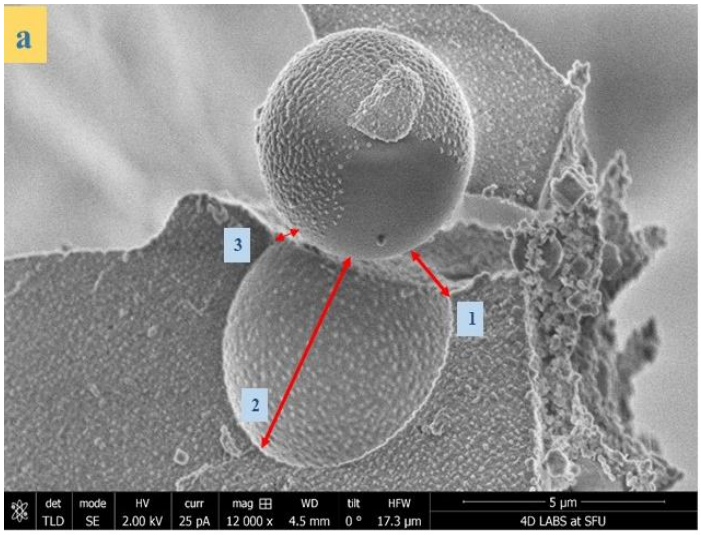

252 **Sample before sublimation (-180 °C)**

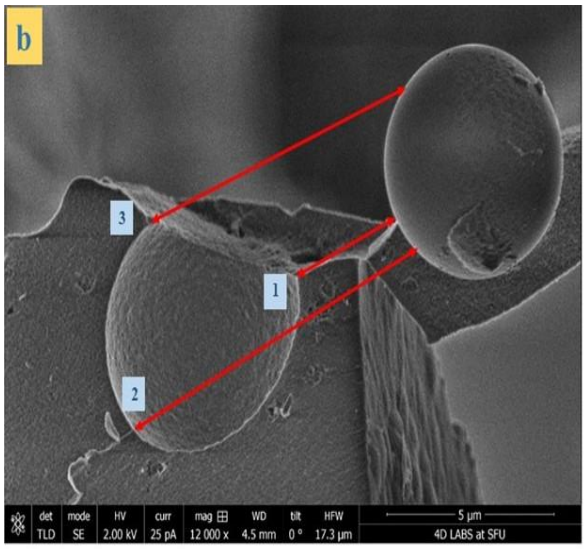

Sample after sublimation (-70 °C)

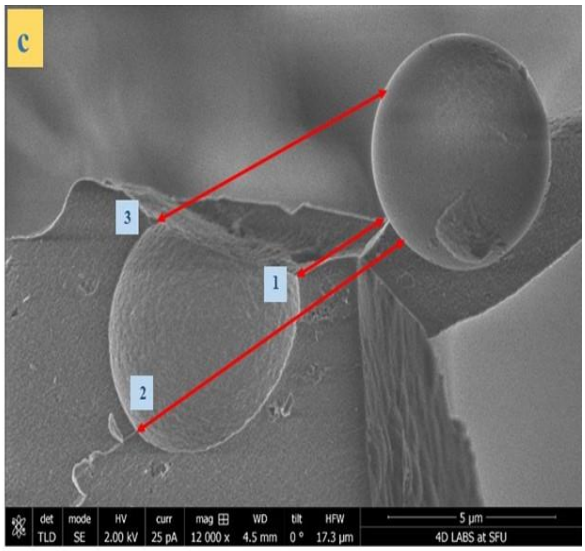

253 **Sample after sublimation (-10 °C)**

254 **Figure 6. 4D-LTSEM images of by-product particle at following temperatures: (a) -180 °C, (b) -70 °C and (c) -10°C**

255 Figure.6 also shows sublimation process of ice crystals of GPC from temperature of -180 ºC to
256 -10 ºC. It is obvious that ice totally covered the paste at a temperature of -180 ºC (Figure.6 (a))
257 and ice was dramatically sublimated from surface of paste by decreasing temperature from
258 -180 ºC to -70 ºC (Figure.6 (b)). Eventually, most amount of ice sublimated from the paste at
259 a temperature of -10 ºC (Figure.6 (c)). However, Figure.6 also shows that the rate of ice
260 sublimation between -70 ºC to -10 ºC is higher compared to rate of cryo products sublimation
261 between -180 ºC to -70 ºC. So, it shows that GPC is frost resistant up to -70 ºC.

262 D.J. Corr (Corr, et al., 2002) proposed that contact angles between cryo products and air void
263 wall is a significant parameter to be measured because it affects the hydraulic pressure of the

capillary pores during the freezing of water. However, in this study, it is found that cooling temperature also causes by-products particle to move apart from paste. An image (magnification of 12K) from one particle was taken to measure the distance of the particle from three reference points (1, 2, 3). Table. 3 indicates that the average distance of the particle at -180 ºC (Figure.6 (a)) is 2.18 µm. However, when the temperature increased from -180 ºC to -70 ºC, the average distance of the particle increased from 2.18 µm to 6.68 µm. Table. 3 also shows that there is no considerable change in distance when temperature increased from -70 ºC to -10 ºC.

Table 3- Distance measurements

Figure.6 code	N0.	Distance (µm)	Average (µm)
a	1	1.29	2.18
	2	4.89	
	3	0.38	
b	1	3.24	6.68
	2	9.19	
	3	7.63	
c	1	3.25	6.69
	2	9.21	
	3	7.63	

Generally, it is reported that elevated curing temperature is helpful toward dissolution of by-products particle (Patil, et al., 2014) (Ken, et al., 2015). GPC requires heat treatment in order to obtain high compressive strength. It means higher curing temperature results in higher interfacial transition zone bonding. In contrast, Pilehvar et al. (Pilehvar, et al., 2019) proposed that frost actions cause microcracks initiation and bonding strength loss at the weak interfacial transition zone.

Figure.6 and measured distance (Table.3) show that by-product particle located on an air void at temperature of -180 ºC. However, after sublimation to -70 ºC, the particle moved away from its location. This phenomenon also can be explained with bonding strength of paste at lowest temperature. At temperature between 0 ºC to -70 ºC, most likely bonding strength of GPC was higher than that at temperature of -180 ºC and only freezing of water in larger pores was predominant. However, the bonding strength of the paste decreased at a temperature between -70 ºC to -180 ºC and probably freezing of water in smaller pores was predominant due to the

drop of freezing point of the capillary water. In this study, the distance between the particle and matrix decreased with the increasing temperature from -180 ºC to -10 ºC. Generally, at large distances, the strength reduces, meaning that there is no interaction between particles. At short distances between the two particles, due to attraction force, and chemical tendency of particles to create a polymer/covalent bond, the bond strength between particles is very high.

5. Conclusion

In this paper, K-based GPC as a sustainable material was developed to investigate the microstructure of cryo products structure in the air voids of paste. A new technique was also used to maintain the temperature as low as possible to capture morphology of cryo products propagation in the air void of GPC. The results indicate that:

1- The SEM image of K-based GPC shows that due to full and uniform curing process, most proportation of fly-ash and bottom-ash reacted with alkaline solution and created a dense matrix.
2- Investigation of cryo formation in the air voids of GPC showed that the cryo non-discretely covered the surface of air void because the specimen were fully-saturated. This is not in full agreement with literature where cryo formation in the air voids of PCC indicated discrete and hemispheric cryo crystals along the wall of air voids.
3- Microstructure investigation of cryo products showed that cryo products covered GPC at temperature of -180 ºC but most amount of cryo products was sublimated at a temperature of -70 ºC. Finally, a few amount of cryo products was observed on surface of the paste at a temperature of -10 ºC. However, it was found that the rate of cryo products sublimation between -180 ºC to -70 ºC was high. While, due to frost resistance of GPC upto -70 ºC, there was no significant sublimation rate when temperature changed from -70 ºC to -10 ºC.
4- Distance measurement of GPC was performed to investigate the effect of cooling temperature on the bonding strength of the paste. The average distance measurement of particle at -180 ºC, -70 ºC, and -10 º C showed that the average distance of the particle at -180 ºC was 2.18 μm. However, by increasing temperature from -180 ºC to -70 ºC, the average distance of the particle increased from 2.18 μm to 6.68 μm. It was also observed that there was no significant change in distance when sublimation process occurred from -70 ºC to -10 ºC. So, it can be noticed that GPC has reasonable bonding strength up to -70 ºC.

Acknowledgment

The authors would like to acknowledge the financial supports from India-Canada Research Centre of Excellence (IC-IMPACTS), as well as extend their appreciation to Xin Zhang, lab technician in 4D LABS (Materials Science Research Institute) of Simon Fraser University. Authors also appreciate the discussion and comments from Dr. Elaine Humphrey, lab manager at Advanced Microscopy Facility of University of Victoria.

References

ASTM C231/C231 M-15, 2015. Standard Test Method for Air Content of Freshly Mixed Concrete by the Pressure Method, Annual Book of ASTM Standard, Philadelphia.

ASTM C666/C666 M-15, 2015. Standard test method for resistance of concrete to rapid freezing and thawing, Annual Book of ASTM Standard, Philadelphia.

Azarsa, P. & Gupta, R., 2018. Specimen preparation for nano-scale investigation of cementitious repair material. Micron, Volume 107, pp. 43-45.

Bakharev, T., Sanjayan, J. & Cheng, Y.-B., 2000. Effect of admixtures on properties of alkali-activated slag concrete. Cement and Concrete Research , Volume 30, pp. 1367-1374.

Belforti, F., Azarsa, P., Gupta, R. & Dave, U., 2017. Effect of Freeze-Thaw on K-based Geopolymer Concrete and Portland Cement Concrete. India, 6th Nirma University international conference on engineering, NUiCONE 2017.

Chindaprasirt, P., Jaturapitakkul, C., Chalee, W. & Rattanasak, U., 2009. 4. Prinya Chindaprasirt , Chai Jaturapitakkul , WiComparative study on the characteristics of fly ash and bottom ash geopolymers. Waste management, Volume 29, pp. 539-543.

Corr, D. J., Monteiro, P. J. M. & Bastacky, J., 2002. Microscopic Characterization of Ice Morphology in Entrained Air Voids. Aci Materials Journal, Volume 99-M18.

Davidovits, J., 2015. Geopolymer chemistry and application. France : Geopolymere instute, ISBN: 9782951482098.

Gupta, R. & Rathod, H. M., 2015. Current state of K-based geopolymer cements cured at ambient temperature. Emerging Materials Research, 4(1), pp. 125-129.

H.S.Wong, A.M.Pappas, R.W.Zimmerman & N.R.Buenfeld, 2011. Effect of entrained air voids on the microstructure and mass transport properties of concrete. Cement and Concrete Research , Volume 41, pp. 1067-1077.

Hanjitsuwan, S., Phoo-ngernkham, T. & Damrongwiriyanupap, N., 2017. Comparative study using Portland cement and calcium carbide residuevas a promoter in bottom ash geopolymer mortar. Construction and Building Materials , Volume 133, pp. 128-134.

Isac-García Joaquín, A.Dobado José, G.Calvo-Flores Francisco, Martínez-García Henar, 2016. Chapter 10, Microscale. Experimental Organic Chemistry, Lab manual, Pages 353-370.

Kabashi, N., Krasniqi, C., Morina, H. & Dautaj, A., 2016. Effect of Air voids in Fresh and Hardening properties of Concrete. Tirana, Albania, 3rd International Balkans Conference on Challenges of Civil Engineering, 3-BCCCE, Epoka University.

Ken, P. W., Ramli, M. & Ban, C. C., 2015. An overview on the influence of various factors on the properties of geopolymer concrete derived from industrial by-products. Construction and building materials , Volume 77, pp. 370-395.

Kosior-Kazberuka, M. & Berkowskib, P., 2017. Surface scaling resistance of concrete subjected to freeze-thaw cycles and sustained load. Procedia Engineering , Volume 172, pp. 513-520.

Mal'chik, A., Litovkin, S. V. & Rodionov, P. V., 2015. Investigations of physicochemical properties of bottom-ash materials for use them as secondary raw materials. Volume 91, IOP Conf. Series: Materials Science and Engineering.

Mehta, P. K. & Monteiro, P. J., 2014. Concrete microstructure, properties, and materials. 4 ed., ISBN 978-0-0-07-179787-0, USA.

Mohamed, R., Zakaria, H. & Azizli, M. K. A., 2016. Concentration of NaOH and the Effect on the Properties of Fly Ash Based Geopolymer. Procedia Engineering , Volume 148, pp. 189-193.

Monteiro, P. J. M., Coussy, O. & Silva, D. A., 2006. Effect of Cryo-Suction and Air Void Transition Layer on Hydraulic Pressure of Freezing Concrete. Aci Materials Journal, Volume 103-M16.

Patil, A. A., Chore, H. & Dode, P., 2014. Effect of curing condition on strength of geopolymer concrete. Advances in Concrete Construction, 2(1), pp. 29-37.

Pilehvar Shima, M.Szczotok Anna, Rodríguez Juan Francisco, Valentini Luca, Lanzón Marcos, Pamies Ramón, Kjøniksen Anna-Lena, 2019. Effect of freeze-thaw cycles on the mechanical behavior of geopolymer concrete and Portland cement concrete containing micro-encapsulated phase change materials. Construction and building materials. Volume 200, pp.94-103.

Powers, T. C., 1958. The physical structure and engineering propertiesof concrete. Portland Cement Associacition Bulletin, Volume 90, pp. 1-28.

Powers, T. C. & Helmuth, R. A., 1953. Theory of volume changes in hardened Portland cement paste during freezing. Highway Research Board Bulletin, Volume 32, pp. 285-297.

Shang, H.-S. & Yi, T.-H., 2013. Freeze-Thaw Durability of Air-Entrained Concrete. The Scientific World Journal, Volume 2013, p. 650791.

Sun, P. & Wu, H.-C., 2013. Chemical and freeze-thaw resistance of fly ash-based inorganic mortars. Fuel, Volume 111, pp. 740-745.

Wang, K., Monteiro, P. J., Rubinsky, B. & Arav, A., 1996. Microscopic Study of Ice Propagation in Concrete. Aci Materials Journal, Volume 93-M42.

Xie, T. & Ozbakkaloglu, T., 2015. Behavior of low-calcium fly and bottom ash-based geopolymer concrete cured at ambient temperature. Ceramics International, 41(4), pp. 5945-5958.

Yang, C. & Gupta, R., 2018. Prediction of the compressive strength from resonant frequency for low-calcium fly ash-based geopolymer concrete. Journal of Materials in Civil Engineering, Volume 30.

Yu, H., Maa, H. & Yan, K., 2017. An equation for determining freeze-thaw fatigue damage in concrete and a model for predicting the service life. Construction and Building Materials , Volume 137, pp. 104-116.

Yu, J. et al., 2012. Analysis on Characteristics of Fly Ash from Coal Fired Power Stations. Energy Procedia, Volume 17, pp. 3-9.

Ziaei-Nia, A., Tadayonfar, G.-R. & Eskandari-Naddaf, H., 2018. Effect of Air Entraining Admixture on Concrete under Temperature Changes in Freeze and Thaw Cycles. Materials Today: Proceedings , Volume 5, pp. 6208-6216.